Dendrites enable a robust mechanism for neuronal stimulus selectivity

Romain D. Cazé[1,*], Sarah Jarvis [1], Amanda J. Foust[1], Simon R. Schultz[1],

1 Centre for Neurotechnology and Department of Bioengineering, Imperial College London, South Kensington, London, SW7 2AZ, UK

* romain.caze@gmail.com
Keywords: Dendrites — stimulus selectivity — single neuron computation

Abstract

Hearing, vision, touch – underlying all of these senses is stimulus selectivity, a robust information processing operation in which cortical neurons respond more to some stimuli than to others. Previous models assume that these neurons receive the highest weighted input from an ensemble encoding the preferred stimulus, but dendrites enable other possibilities. Non-linear dendritic processing can produce stimulus selectivity based on the spatial distribution of synapses, even if the total preferred stimulus weight does not exceed that of non-preferred stimuli. Using a multi-compartment non-linear model, we demonstrate that selectivity can arise from the spatial distribution of synapses. Moreover, we show that this implementation of stimulus selectivity increases the neuron's robustness to synaptic and dendritic failure. Contrary to an equivalent linear model, our model can maintain stimulus selectivity even when 50% of synapses fail or when more than 50% of dendrites fail. We then use a Layer 2/3 biophysical neuron model to show that our implementation is consistent with recent experimental observations, of a mixture of selectivities in dendrites, that can differ from the somatic selectivity, and of hyperpolarization broadening somatic tuning without affecting dendritic tuning. Our model predicts that an initially non-selective neuron can become selective when depolarized. In addition to motivating new experiments, the model's increased robustness to synapses and dendrites loss provides a starting point for fault-resistant neuromorphic chip development.

Author summary

From the stripes of your shirt to the sound of your grandmother's name, your neurons are capable of selecting among stimuli. How do they perform this selection? The standard model assumes that a neuron receives the strongest inputs from neurons encoding its preferred stimulus. While this can explain many observations, it fails to address recent observations, and neglects dendrites, the neuron's "antenna" for receiving inputs. Here we propose an alternate model for stimulus selectivity which incorporates dendrites fitting with the latest experimental observations and robust to a 50% synapses or dendrites failure. The computational capacity as well as the robustness enabled by dendrites offer new possibilities for neuromorphic chip design.

1   Introduction

Over 50 years ago, Hubel and Wiesel discovered an example of neuronal stimulus selectivity [1], in which certain neurons in the visual cortex respond maximally to particular visual stimuli. They proposed a single compartment model where a neuron linearly sums inputs from cells encoding the preferred orientation. This type of model neglects dendrites, that can enhance a neuron's computational capacity [2,3]. We wish to examine here whether dendrites can also facilitate the implementation of an important biological information processing function such as stimulus selectivity. Moreover, several groups have recently presented data which is counter-intuitive given the Hubel and Wiesel model. Firstly, this model integrates inputs with a narrow range of orientations. In contrast, experimental group observed a mixture of selectivity on all dendritic branches [4,5]. Secondly, it was observed that hyperpolarization can significantly broaden somatic tuning, while dendritic tuning stays sharp [5]. Taken together, these observations call for models more complex than a single linear compartment, and in this paper we propose that they can be accounted for by the properties of dendrites.

2   Results

Dendrites allow stimulus selectivity based on the spatial distribution of synapses

Multiple biophysical studies have demonstrated that dendrites render a neuron's output sensitive to the spatial distribution of synapses [6,7]. We propose here a novel possible implementation of stimulus selectivity using this sensitivity. In our non-linear model (presented in Methods), each dendritic compartment processes its input independently with the same transfer function (Fig. 1A), as in real neurons [8–11]. Even without dendritic spiking ($d=1$), a compartment integrates synaptic input non-linearly, i.e. sub-linearly, as it reaches a plateau when synaptic input overshoots θ. According to the spatial distribution of synapses activated, these non-linearities will give rise to stimulus selectivity. When more than a certain number of synapses activate on a single branch (one hundred in our simulations), a dendritic threshold θ is exceeded, and the compartment saturates. When synaptic inputs are scattered across the dendritic tree, however, multiple compartments reach maximum depolarization together, potentially leading to the neuron exceeding its threshold for firing. The crucial aspect of our implementation of stimulus selectivity is that different stimuli lead to different spatial patterns of synaptic activation, with the "preferred" stimulus for a neuron leading to activation of a spatially scattered set of synapses (Fig. 1B-C).

We computed the dendritic activity in our model, including seven compartments on which nearly 5000 synapses ($n = 4950$) are distributed. These synapses come from 8 different neuronal ensembles, with each ensemble coding for a different stimulus. The ensemble coding for the preferred stimulus targets all dendritic compartments (700 synapses), whereas the ensembles coding for the non-preferred stimuli each tended to cluster 40% of their synapses (n=650) onto a single dendritic compartment. The remaining synapses are then distributed randomly among all other dendritic compartments. We describe this distribution in Table.1 and graphically in Fig.1C-D.
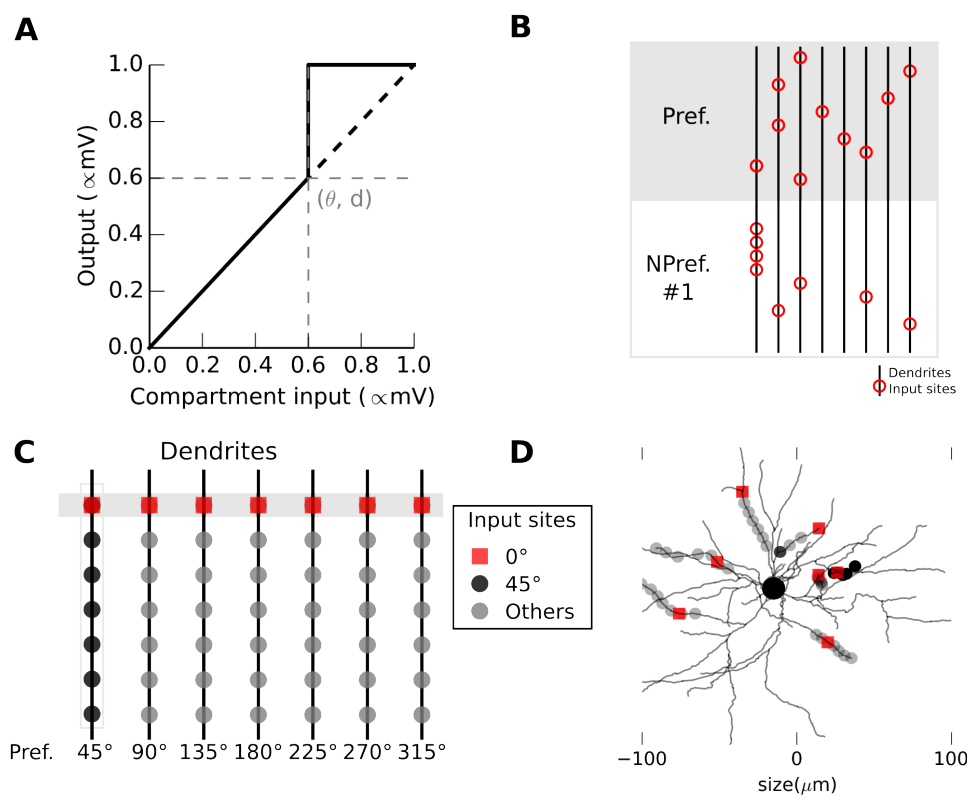
Figure 1. Non-linearities enable stimulus selectivity using the spatial distribution of synapses. (A) Local transfer function in a dendritic compartment; a non-linear jump occurs at the point (θ, d). Input and output are normalized given their respective maxima. (B) The input sites (red circles) on dendrites (horizontal lines) are where the highest number of synaptic contacts are made (at most 70 synapses). The preferred stimulus (Pref.) makes the highest number of synapses and the most scattered distribution. (C-D) Schematic depiction of the spatial distribution of synapses on dendrites (red: preferred 0, black/gray: non-preferred from 45 to 315). (C) Each compartment displays distinct selectivity. Pref (shaded area) and NPref are respectively scattered or clustered. (D) The synaptic distribution on a realistic reconstruction of a L2/3 neuron.
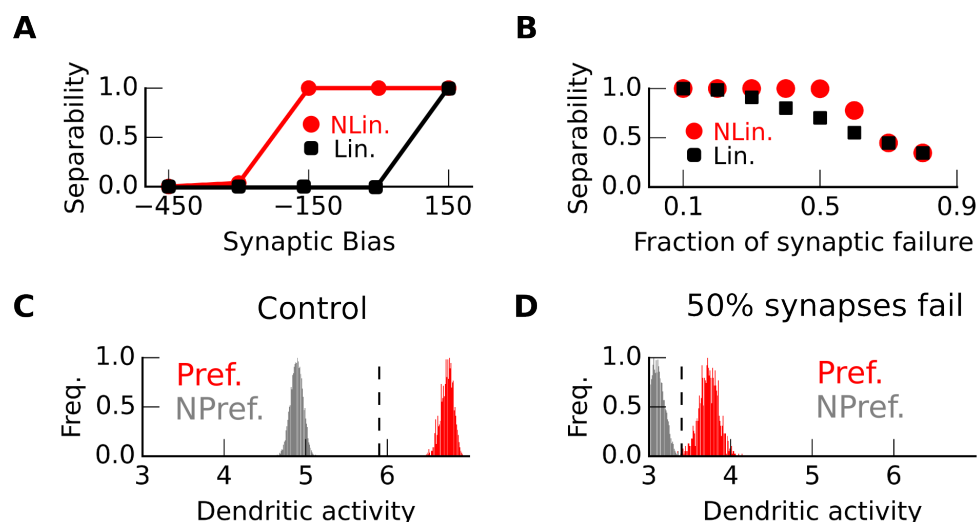
Figure 2. Stimulus selectivity achieved with the spatial distribution of synapses increases the robustness to synaptic failure. (A-B) Separability, calculated as the fraction of random model instances capable of separating preferred and non-preferred stimuli ($n = 1000$), for the non-linear (red circles) and linear (black square) model as a function of (A) the synaptic bias, which is the difference in the number of synapses between preferred and non-preferred ensemble; or (B) the synaptic failure which is the fraction of malfunctioning synapses. (C-D) Distribution of dendritic activity in number of compartments maximally active for preferred (red) and non-preferred stimuli (gray) in the non-linear models. (C) In control condition, or (D) with 50% synapses failing.

Spatial distribution based stimulus selectivity increases robustness to synaptic and dendritic failure

In this section, we probe the robustness of our implementation by comparing two multi-compartmental models in which integration in compartments is either non-linear (θ typically equal to $\frac{1}{7}$ and $d=1$) or linear ($\theta=1$ and $d=1$).

In a linear model it is necessary that the preferred ensemble makes the strongest contact. A linear model stops being stimulus selective when a non-preferred stimulus makes stronger contacts than the preferred stimulus (Fig. 2A, black), for which proof is given in Methods. Our non-linear model remains stimulus selective even when the preferred stimulus ensemble forms 200 fewer synapses than non-preferred stimulus ensembles (Fig. 2A, red). This property of our non-linear model confers robustness against synaptic failure (Fig. 2B), where a synapse stays inactive when it should be active. It can separate both types of stimulus (Fig. 2C) and can maintain its function after 50% of its synapses fail (Fig. 2D).

The implementation using a non-linear model also maintains its function when dendrites are disabled. A non-linear model can select stimuli even if only 10% of synapses have a fixed position (Fig. 3A red). This considerably boosts the stability of the non-linear model, which can maintain functionality even under the loss of more than 50% of compartments (Fig. 3B black and Fig. 3C). In comparison, a linear model cannot use the spatial distribution of synapses and if the synaptic bias is nil, it is impossible to differentiate preferred and non-preferred stimuli (Fig. 3A black). The clustering bias (here 30 %) is detrimental for this type of model. It makes the linear model sensitive to the loss of even a single compartment (Fig. 3B black). Fig. 3D shows
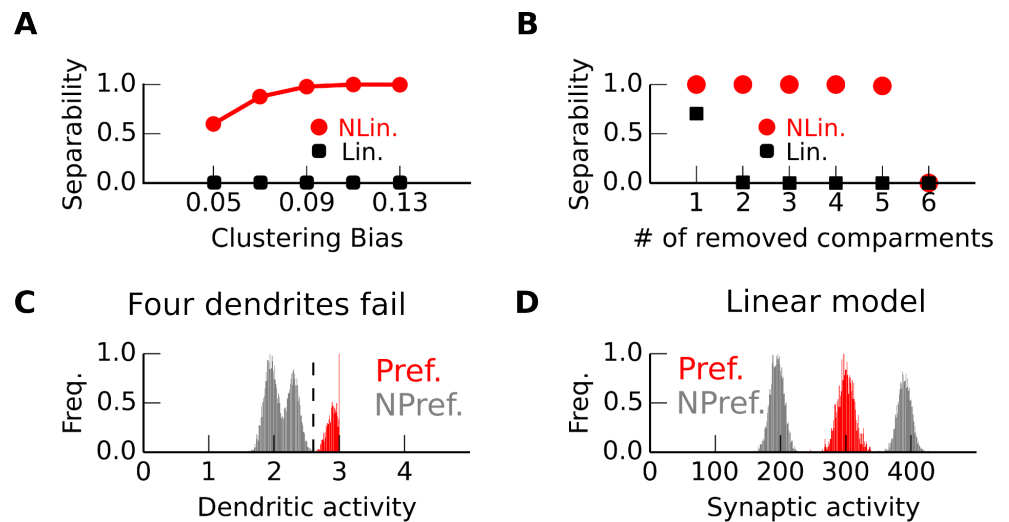
Figure 3. Stimulus selectivity achieved with spatial distribution of synapses increases the robustness to dendritic failure. (A-B) Separability, calculated as the fraction of models capable of separating preferred and non-preferred stimuli ($n = 1000$), for the non-linear (red circles) and linear (black square) model as a function of (A) the clustering bias, which is the number of synapses specifically set on a precise compartment; and (B) the number of removed compartments. (C-D) Distribution of dendritic activity for preferred (red) and non-preferred (gray) (C) in the non-linear models where dendritic activity closely relates to the number of maximally active compartment; and (D) in the linear model, where synaptic activity is the number of active synapses.

that it is impossible for a linear model losing four dendrites to separate the preferred and non-preferred stimuli.

In summary, we compared two multi-compartmental models: a linear and a non-linear model. We used simulations to demonstrate that the non-linear model is much more robust than its linear equivalent. Our non-linear multi-compartmental model can lose 50% (more than 2600) of its synapses or more than 50% of its dendrites (more than 4) while maintaining stimulus selectivity.

The biophysical model replicates the mixture of dendritic tunings

We have shown how a multi-compartment non-linear model can robustly implement stimulus selectivity. The following section demonstrates that these results carry over to a biophysical model capturing rich temporal dynamics and interactions between compartments. This biophysical model fits recent experimental observations [5].

We constructed a stimulus selective neuron (Fig. 4A) that replicates the experimental data. Both the data and our model can display a variety of dendritic tunings (Fig. 4B-C). To replicate the experimental observations, we used 8 ensembles of AMPA/NMDA-type synapses distributed each on 7 locations. Synapses from the preferred stimulus ensemble scatter across all branches, whereas synapses from the non-preferred ensembles cluster, each onto a particular dendrite. We placed these synapse on a Layer 2/3 neuron reconstruction [5] (Fig. 1D).

The activation of a synapse results in a somatic depolarization of $\frac{1}{7}$ mV, independent of its location, as observed in [12] Fig. 4C). We enforced this "dendritic democracy" [13]
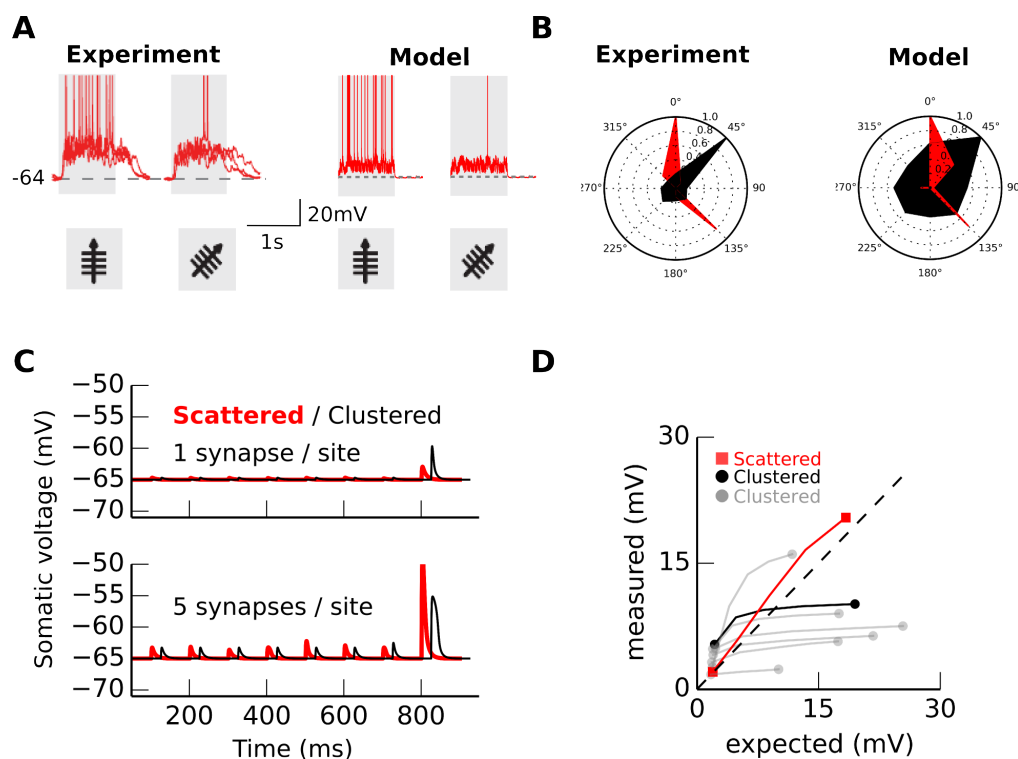
Figure 4. Stimulus selectivity implemented through the spatial distribution of synapses displays a mixture of dendritic selectivities. (A) Somatic voltage for two stimuli (0/45 degrees during shaded period). (B) Spike count (red) and selectivity in dendrites (one example; black, calcium signal integral). (C) Somatic depolarization when one(top)/five(bottom) synapse(s) activate in one of the input sites from 0 to 800 ms; or when one/five occurs at all the 7 sites (800 to 1000ms). Input locations are described in Fig. 1 (red: scattered/black: clustered). (D). Expected (arithmetic sum) versus measured depolarization in the simulated 2 sets of 7 locations.

by scaling synaptic conductances depending on their distance to the soma. Each ensemble makes the same number of synapses, so all ensembles contact the post-synaptic neuron with the same strength if we sum arithmetically all synaptic weights.

Interestingly, synapses interact in two distinct ways, dependent on their location. For synapses clustered on a branch (Fig. 4C, black trace), seven active synapses (one per location) interact supra-linearly and they produce a depolarization superior to one mV because they generates an NMDA spike [14], but 35 synapses (five per location) interact sub-linearly due to reduced driving force at synapses [7, 15]. In contrast, for synapses scattered across the seven branches, synapses interact linearly (Fig. 4C, red trace) as has been observed experimentally *in vivo* [16]. These observations are summarized in an expected/measured plot (Fig. 4D) and show the biophysical model's sensitivity to the synaptic spatial distribution.

This sensitivity enables the generation of stimulus selectivity in our model. If the population coding for the preferred stimulus makes functional synapses on all primary dendrites, whereas non-preferred stimuli cluster on single branches, then the distributed synaptic arrangement produces multiple NMDA spikes that reach the soma in parallel, as observed *in vitro* [17] and *in vivo* [18, 19] (Fig. 4A). Both scenarios are illustrated in animations provided as supplementary material (see movies S1 and S2).

In a single compartment model, the highest weighted stimulus always "wins",

rendering synaptic spatial distribution irrelevant. Conversely, our multi-compartment biophysical model uses exclusively the spatial distribution of synapses to implement stimulus selectivity, a configuration that could explain, in contrast with single compartment models, how calcium hotspots in dendrites display mixed stimulus tuning [5].

Hyperpolarization broadens somatic but sharpens dendritic tuning in our model

We injected current at the soma in our biophysical model to pull down the membrane potential from -64mV to -70mV, as in Jia et al.'s experiment [5]. In this case, the neuron stops firing action potentials, however, hyperpolarization also affects the shape of the subthreshold potential both in soma and dendrites.

When we decrease the resting membrane voltage to -70mV, the number of synapses necessary to trigger an NMDA spike increases, and only the dendritic preferred stimulus provokes an NMDA spike. Fig. 5A shows that only the 45 degree stimulus triggers dendritic spikes, and dendritic selectivity sharpens (Fig. 5B). Conversely, the somatic depolarization difference between scattered and clustered synapses decreases, when we hyperpolarize the neuron (Fig. 5C-D), and somatic selectivity broadens.

The model's sensitivity to the spatial distribution of synapses can thus explain the differential effect of hyperpolarization on somatic and dendritic tuning.

3   Discussion

Local and non-linear integration could have made our model cluster sensitive. Instead it responds more to scattered (widely distributed) synaptic activity. This behavior had previously been described [6,7], but has never been proposed as a mechanism underlying stimulus selectivity. Recent unexpected experimental observations [5] have motivated our usage of scatter sensitivity, rather than cluster sensitivity, for this purpose. Additional experimental work, for instance where dendrites are disabled using targeted laser dendrotomy [20], will however be necessary to confirm the functional role of scatter sensitivity.

We implemented stimulus selectivity in a multi-compartment non-linear model (Fig. 1) that can lose 50% synapses or more than 50% of its dendrites and maintain stimulus selectivity (Fig. 2). Importantly, the selectivity mechanism we propose can coexist with a classical mechanism based upon synaptic strength (Fig. 4A), providing an additional channel for neuronal information processing. In practice, the preferred ensemble does make the strongest contact, as observed recently by Chen et al [21]. A linear model can also be robust if there is a large difference in the number of synapses between preferred and non-preferred ensembles. In our study, we used the same synaptic difference in both models to show that using the spatial distribution of synapses adds to any existing robustness.

Although we have focused, to ease comparison with experimental studies, on the tuning of a neuron to sensory stimuli, all neural computations can be described in terms of stimulus selectivity. Boolean functions can both describe a neural computation and stimulus selectivity. In the latter case, we can describe preferred stimuli and non-preferred stimuli as words of 0s and 1s. In the former case, we can describe all neural computations as Boolean functions if we binarize activity. Therefore our implementation based on the spatial distribution of synapses can be used for general neural computation. To transpose a synaptic strength based implementation of an information processing operation, it suffices to change the strength/overall weight given to an input into a dispersion factor.
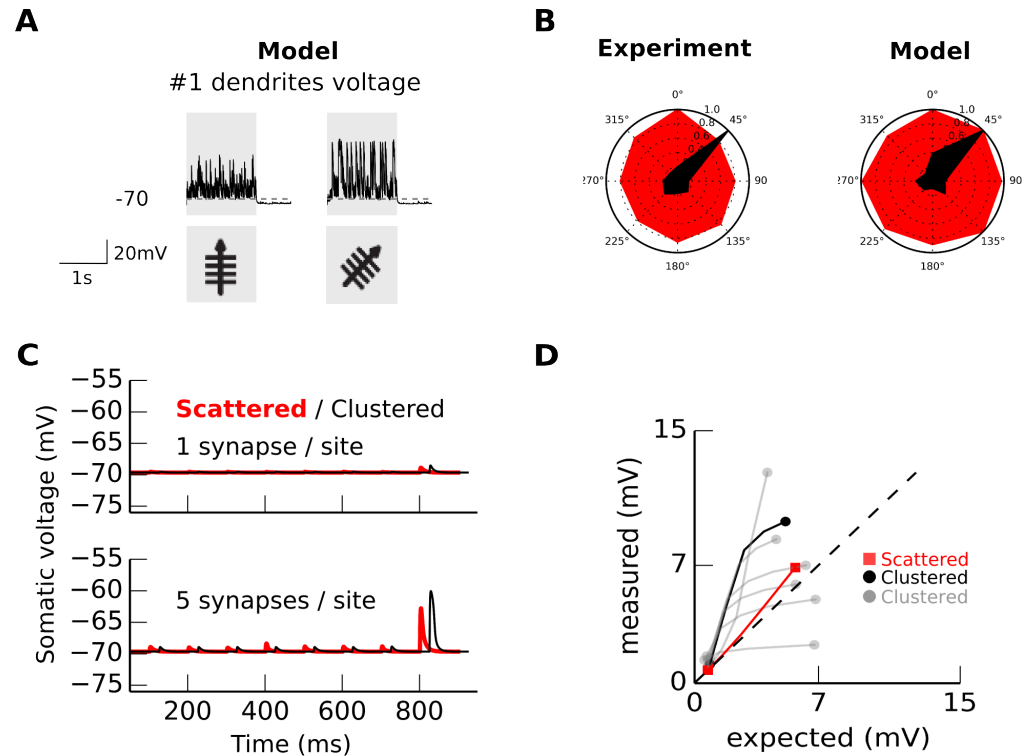
Figure 5. Hyperpolarization broadens somatic tuning whereas it sharpens dendritic tuning in our model. (A) Local membrane potential in the first dendritic branch for two stimuli: the soma's preferred stimulus and for the dendrite's preferred stimulus. (B) Integral of somatic membrane potential in an experiment (replotted from [5]) and in our model. (C) Somatic depolarization when one(top)/five(bottom) synapse activate in one of the input site from 0 to 800 ms; or when one/five occurs at all the 7 sites (800 to 1000ms). Input locations are described in Fig. 1 (red: scattered/black: clustered). (D). Expected (arithmetic sum) versus measured depolarization in the simulation 2 sets of 7 locations.

The biophysical model reinforces that the insights gained from our elementary model are physiologically relevant, and can capture several recent experimental observations, specifically, that (A) stimulus-selective cells receive inputs coding for a variety of stimuli [4, 5] (Fig. 4) and, (B) hyperpolarization broadens somatic tuning [5, 22] while it sharpens dendritic tuning (Fig. 5). Our results, taken together, make two testable predictions. Firstly, our model predicts that a neuron may recover its tuning after losing a large fraction of either its synapses or dendrites, due to the robustness provided by spatial synaptic distribution based information processing. Secondly, it predicts that a cortical neuron with no apparent stimulus tuning can acquire stimulus selectivity when depolarized, similar to what can be observed in place cells [23].

Our implementation using nonlinear dendritic integration may inform the design of neuromorphic chips, as it suggests that the use of dendrites – even passive – can extend the robustness of the circuit. Dendrites may not only increase the computational power of each unit [3], but also increase their resilience, addressing a crucial issue in the design of fault-tolerant chip architectures. While we have demonstrated these capabilities in the context of a neuron's selectivity to a visual stimulus, the model we have proposed is general, and potentially reflects a canonical computational principle for neuronal information processing.

4   Methods

Multi-compartmental model

Our multi-compartmental model consists of seven dendrites, each receiving input from eight presynaptic neuronal ensembles corresponding to eight different stimulus orientations. The mean number of synaptic contacts for each ensemble-dendrite pair is described in Table 1. The preferred stimulus (0 degrees) activates 700 synapses following a random uniform distribution across all seven dendrites. In contrast, non-preferred stimuli activate 650 connections each, including a bias such that 40% of input from each orientation preferentially target one of the dendrites and the remaining 60% being uniformly distributed among the remaining six dendrites following a uniform distribution. A dendrite saturates when 100 of its synapses are active, and the somatic output will be determined by the arithmetic sum of all the dendritic output.

Table 1. Synaptic distribution in our multi-compartmental model. Mean number of synapses made by each presynaptic ensemble for each stimulus, for each postsynaptic dendrite.

Preferred orientation	Dendrite (d_j)							Total
	0	1	2	3	4	5	6	
0	100	100	100	100	100	100	100	700
45	260	65	65	65	65	65	65	650
90	65	260	65	65	65	65	65	650
135	65	65	260	65	65	65	65	650
180	65	65	65	260	65	65	65	650
225	65	65	65	65	260	65	65	650
270	65	65	65	65	65	260	65	650
315	65	65	65	65	65	65	260	650

A necessary condition for the linear model

The highest weight needs to be from the preferred stimulus in a linear model. To prove that let us consider the simplest scenario where two presynaptic neurons each synapse

onto a postsynaptic neuron. We arrange it so that one input codes for the preferred stimulus while the other for a non-preferred stimulus, and W_{pref} and W_{nonpref} is the amplitude of their resulting depolarization on the postsynaptic neuron. Here, stimulus selectivity is possible only if $W_{\mathrm{pref}} \geq \Theta$ and $W_{\mathrm{nonpref}} < \Theta$, which is equivalent to $W_{pref} > \Theta > W_{\mathrm{nonpref}}$. This condition can be generalized for any number of presynaptic neurons, and implies in the linear neuron model when constrained to positive values of W that stimulus selectivity is only possible when the preferred stimulus has the highest weight.

Synaptic inputs to the biophysical model

We generated 280 presynaptic neurons divided into 8 sets of 35 neurons, corresponding to 8 different orientations. Each had a background firing rate of 1 Hz which increased to 10Hz during the presentation of the stimulus. As experimental evidence suggests that stimulus information is coded not only by an increase in firing rate but also in spike-time correlation [24, 25], we inserted 20 synchronous spikes to the spiketrains from neurons encoding the preferred stimulus, raising their firing rate to 30 Hz.

Conductance based NMDA-type synapses

NMDA-like inputs were included by modelling voltage-dependent, conductance-based synapses that generated postsynaptic currents $i_s = g(t)g_{\mathrm{mg}}(v) \times (v(t) - e_s)$, with reversal potential $e_s =0$ mV. For $g(t)$, we used an alpha-function with rise and decay time constants $\tau_1 = 0.1$ms and $\tau_2 = 10$ms respectively. Values for τ_1 and τ_2 were chosen to be deliberately lower than those for real glutamate binding on NMDA channels to account for the presence of voltage-gated calcium dependent potassium channels in the membrane. The voltage-dependent conductance $g_{mg}(v)$ was determined assuming $[\mathrm{Mg}^{2+}] =1$mM (see .mod file).

physical model

For detailed modelling, we used a reconstructed morphology of a neuron from Layer 2/3 of visual cortex in mouse [5]. The axial resistance in each section was $R_a = 35.4\Omega$, and passive elements were included ($g_l = 0.001 \ \Omega^{-1}$, $e_l = -65$ mV). Spiking was implemented using an integrate-and fire mechanism with a hard threshold of -45mV, which has been shown to provide an accurate depiction of spike initiation behaviour [26], whereupon we set the voltage to 20 mV in the following timestep, before resetting to -65 mV. The model was implemented using NEURON with a Python wrapper [27], with the time resolution set to 0.1ms.

Supporting Information

S1 Video

Neuron response to clustered synaptic inputs. L2/3 neuron reconstruction from the visual cortex. The large circle is the soma and black dots are input sites. Depolarization of a section is color-coded (black:low, yellow:high).

S2 Video

Neuron response to scattered synaptic inputs. L2/3 neuron reconstruction from the visual cortex. The large circle is the soma and black dots are input sites. Depolarization of a section is color-coded (black:low, yellow:high).

Acknowledgments   231

References

1. Hubel DH, Wiesel TN. Receptive fields of single neurones in the cat's striate cortex. The Journal of Physiology. 1959;148:574–591.

2. Cazé RD, Humphries M, Gutkin B. Passive Dendrites Enable Single Neurons to Compute Linearly Non-separable Functions. PLoS Computational Biology. 2013;9(2).

3. Cazé RD, Humphries M, Gutkin BS. Spiking and saturating dendrites differentially expand single neuron computation capacity. Advances in neural information processing systems. 2012;25:1–9. Available from: http://books.nips.cc/papers/files/nips25/NIPS2012{_}0519.pdf.

4. Smith SL, Smith IT, Branco T, Häusser M. Dendritic spikes enhance stimulus selectivity in cortical neurons in vivo. Nature. 2013;503(7474):115–20. Available from: http://www.ncbi.nlm.nih.gov/pubmed/24162850.

5. Jia H, Rochefort NL, Chen X, Konnerth A. Dendritic organization of sensory input to cortical neurons in vivo. Nature. 2010;464(7293):1307–1312. Available from: http://www.nature.com/doifinder/10.1038/nature08947.

6. Mel BW. Synaptic integration in an excitable dendritic tree. Journal of Neurophysiology. 1993;70(3):1086–101. Available from: http://www.ncbi.nlm.nih.gov/pubmed/8229160.

7. Koch C, Poggio T, Torres V. Retinal ganglion cells: a functional interpretation of dendritic morphology. Phil Trans R So Lond B. 1982;298(1090):227–263. Available from: http://rstb.royalsocietypublishing.org/content/298/1090/227.short$\delimiter"026E30F$nhttp://rstb.royalsocietypublishing.org/cgi/doi/10.1098/rstb.1982.0084.

8. Polsky A, Mel BW, Schiller J. Computational subunits in thin dendrites of pyramidal cells. Nature Neuroscience. 2004;7(6):621–627. Available from: http://www.ncbi.nlm.nih.gov/pubmed/15156147.

9. Tamás G, Szabadics J, Somogyi P. Cell type- and subcellular position-dependent summation of unitary postsynaptic potentials in neocortical neurons. Journal of Neuroscience. 2002;22(3):740–747. Available from: http://www.ncbi.nlm.nih.gov/pubmed/11826103.

10. Abrahamsson T, Cathala L, Matsui K, Shigemoto R, DiGregorio DA. Thin Dendrites of Cerebellar Interneurons Confer Sublinear Synaptic Integration and a Gradient of Short-Term Plasticity. Neuron. 2012;73(6):1159–1172. Available from: http://linkinghub.elsevier.com/retrieve/pii/S0896627312001821.

11. Cash S, Yuste R. Input summation by cultured pyramidal neurons is linear and position-independent. The Journal of Neuroscience. 1998;18(1):10–15. Available from: http://www.ncbi.nlm.nih.gov/pubmed/9412481.

12. Smith MA, Ellis-Davies GCR, Magee JC. Mechanism of the distance-dependent scaling of Schaffer collateral synapses in rat CA1 pyramidal neurons. The Journal of Physiology. 2003;548(1):245. Available from: http://www.jphysiol.org/cgi/doi/10.1113/jphysiol.2002.036376http://jp.physoc.org/content/548/1/245.short.

13. Häusser M. Synaptic function: Dendritic democracy. Current Biology. 2001;11(1):R10–R12. Available from: http://linkinghub.elsevier.com/retrieve/pii/S0960982200000348.

14. Nevian T, Larkum ME, Polsky A, Schiller J. Properties of basal dendrites of layer 5 pyramidal neurons: a direct patch-clamp recording study. Nature. 2007;200(2):7. Available from: http://www.nature.com/doifinder/10.1038/nn1826http://www.physio.unibe.ch/dendrites/PDFs/Nevian{_}2007{_}NatNeurosci.pdf.

15. Tran-van Minh A, Cazé RD, Abrahamsson T, Cathala L, Gutkin BS, DiGregorio DA. Contribution of sublinear and supralinear dendritic integration to neuronal computations. Frontiers in Cellular Neuroscience. 2015;9(March):1–15.

16. Jia H, Varga Z, Sakmann B, Konnerth A. Linear integration of spine Ca2+ signals in layer 4 cortical neurons in vivo. Proceedings of the National Academy of Sciences of the United States of America. 2014;111(25):9277–82. Available from: http://www.ncbi.nlm.nih.gov/pubmed/24927564.

17. Larkum ME, Waters J, Sakmann B, Helmchen F. Dendritic spikes in apical dendrites of neocortical layer 2/3 pyramidal neurons. The Journal of Neuroscience. 2007;27(34):8999–9008. Available from: http://www.ncbi.nlm.nih.gov/pubmed/17715337.

18. Hill DN, Varga Z, Jia H, Sakmann B, Konnerth A. Multibranch activity in basal and tuft dendrites during firing of layer 5 cortical neurons in vivo. Proceedings of the National Academy of Sciences. 2013;110(33):13618–13623.

19. Palmer LM, Shai AS, Reeve JE, Anderson HL, Paulsen O, Larkum ME. NMDA spikes enhance action potential generation during sensory input. Nature Neuroscience. 2014;17(3):383–90. Available from: http://www.ncbi.nlm.nih.gov/pubmed/24487231.

20. Go MA, Choy JMC, Colibaba AS, Redman S, Bachor HA, Stricker C, et al. Targeted pruning of a neuron's dendritic tree via femtosecond laser dendrotomy. Scientific reports. 2016;6:19078.

21. Chen TW, Wardill TJ, Sun Y, Pulver SR, Renninger SL, Baohan A, et al. Ultrasensitive fluorescent proteins for imaging neuronal activity. Nature. 2013;499(7458):295–300. Available from: http://www.ncbi.nlm.nih.gov/pubmed/23868258.

22. Lavzin M, Rapoport S, Polsky A, Garion L, Schiller J. Nonlinear dendritic processing determines angular tuning of barrel cortex neurons in vivo. Nature. 2012;490(7420):397–401. Available from: http://www.nature.com/doifinder/10.1038/nature11451.

23. Lee D, Lin BJ, Lee AK. Hippocampal place fields emerge upon single-cell manipulation of excitability during behavior. Science. 2012;337(6096):849–53. Available from: `http://www.ncbi.nlm.nih.gov/pubmed/22904011`.

24. Bruno RM, Sakmann B. Cortex is driven by weak but synchronously active thalamocortical synapses. Science. 2006;312(5780):1622–7.

25. DeCharms RC, Merzenich MM. Primary cortical representation of sounds by the coordination of action-potential timing. Nature. 1996;381:610–613.

26. Brette R. What Is the Most Realistic Single-Compartment Model of Spike Initiation? PLoS Computational Biology. 2015;11(4).

27. Hines ML, Davison AP, Muller E. NEURON and Python. Frontiers in Neuroinformatics. 2009;3(January):1.